

# Optimizing Fluorescence Detection in Chemical Separations for Analyte Bands Traveling at Different Velocities

Jason B. Shear,<sup>†</sup> Rajeev Dadoo,<sup>†</sup> Harvey A. Fishman,<sup>†</sup> Richard H. Scheller,<sup>‡</sup> and Richard N. Zare<sup>\*†</sup>

Department of Chemistry and Department of Molecular and Cellular Physiology, Howard Hughes Medical Institute, Stanford University, Stanford, California 94305

In many separation techniques, such as field flow fractionation, liquid chromatography, and electrophoresis, chemical species form bands that migrate at distinct velocities. If these bands are to be quantified on-line using a shot-noise-limited detection system, then attention must be given to the data-digitization rate and to the removal rate of molecules from the analyte pool as a result of the detection process. A theory is developed for calculating the signal-to-noise ratio under such conditions, and it is specialized to the case of fluorescence detection in capillary electrophoresis. Using standard detection procedures in which the data-digitization rate and excitation intensity remain constant for the duration of a separation, detection sensitivity can vary by more than a factor of five for bands that arrive at the detection zone between migration times  $\tau_{fast}$  and  $10\tau_{fast}$ , where  $\tau_{fast}$  is the time after the start of the separation that the fastest migrating band arrives at the detection zone. To compensate for different band velocities, both the data-digitization rate and the excitation intensity must be decreased as separation time ( $\tau$ ) increases by the factor  $\tau_{fast}/\tau$ . Only when these corrections are made can uniform sensitivity with the highest possible signal-to-noise ratio be achieved for each peak. These predictions are experimentally tested and compare favorably to observations.

## INTRODUCTION

Historically, most electrophoretic and chromatographic separation techniques have employed *off-line* detection systems. Detection in high-performance liquid chromatography is typically performed in a postcolumn flow cell. In slab gel electrophoresis, measurement of the bands is often accomplished by staining the gel after electrophoretic separation. Recently, a variety of separation techniques have taken advantage of *on-line* detection to simplify analysis and improve reliability. Smith *et al.*<sup>1</sup> developed a fluorescence system for on-line detection with a polyacrylamide tube gel that measured DNA bands as they migrated past the focus of a laser beam. This procedure eliminated the need for manual analysis and the requirement for running multiple, overlapping gels. A similar approach that used fluorescence detection for slab gel electrophoresis has been described by Middendorf *et al.*<sup>2</sup> Microcolumn procedures capable of separating low-volume samples have employed on-line de-

tection almost exclusively because of the ease of implementation—the separation channel is often made of fused silica and is therefore optically transparent—and the relative difficulty of making off-column plumbing connections with low-volume channels.

The advent of microcolumn separation techniques has placed great demands on detection systems. Because column diameters are typically 100  $\mu\text{m}$  or less, UV absorption often yields inadequate detection limits. Among the various low background techniques, laser-induced fluorescence detection has proved the most sensitive; detection of fewer than 1000 analyte molecules, and at concentrations less than 1 pM, is possible for capillary electrophoresis (CE).<sup>3,4</sup> Despite these impressive developments, little consideration has been given to the effects of disparate band velocities on detection sensitivity. Huang *et al.*<sup>5</sup> noted that for on-line detection with CE, an analyte band passes the detection window at a velocity inversely proportional to the time it arrives after the start of separation, an effect that contributes to an increasing *temporal* width of peaks as separation time increases. The consequences of this broadening on radioisotope detection have been discussed by Pentoney *et al.*<sup>6</sup>

Many factors must be considered in optimizing fluorescence detection systems. A stable excitation source and an efficient photodetector that contributes minimally to the overall noise are both critical. In addition, an optical system that maximizes light collection while discriminating analyte fluorescence from background is indispensable. Less obvious is the role played by excitation intensity. White and Stryer<sup>7</sup> presented a theory addressing laser-induced photoalteration of dyes in flowing streams of different velocities. The prediction that excitation intensity must change proportionally to flow velocity to obtain equivalent photoalteration at all flow velocities was experimentally verified for several fluorescent species. Mathies *et al.*<sup>8</sup> later developed a more comprehensive treatment by considering the effects of both photoalteration and ground-state depletion on the optimization of excitation intensity and excitation time in flowing streams.

For separations in which analyte bands traverse the detection zone at different velocities, significant variability in the detection sensitivity can occur. This effect is shown in Figure 1a,b. Here, fluorescein is electrophoresed in a capillary at two different velocities: (1) a "rapid" velocity of 0.32 mm/s (Figure 1a) and (2) a "slow" velocity of 0.08 mm/s

(2) Middendorf, L. R.; Bruce, J. C.; Bruce, R. C.; Eckles, R. D.; Grone, D. L.; Roemer, S. C.; Sloniker, G. D.; Steffens, D. L.; Sutter, S. L.; Brumbaugh, J. A.; Patonay, G. *Electrophoresis* 1992, 13, 487-94.

(3) Wu, S.; Dovichi, N. J. *Talanta* 1992, 39, 173-8.

(4) Fishman, H. A.; Shear, J. B.; Sweedler, J. V.; Zare, R. N. The Pittsburgh Conference on Analytical Chemistry and Applied Spectroscopy, Mar 9-12, 1992, New Orleans, LA; oral presentation; Abstract 300.

(5) Huang, X.; Coleman, W. F.; Zare, R. N. *J. Chromatogr.* 1989, 480, 95-110.

(6) Pentoney, S. L., Jr.; Zare, R. N.; Quint, J. F. *J. Chromatogr.* 1989, 480, 259-70.

(7) White, J. C.; Stryer, L. *Anal. Biochem.* 1987, 161, 442-52.

(8) Mathies, R. A.; Peck, K.; Stryer, L. *Anal. Chem.* 1990, 62, 1786-91.

<sup>†</sup> Department of Chemistry.

<sup>‡</sup> Department of Molecular and Cellular Physiology.

(1) Smith, L. M.; Sanders, J. Z.; Kaiser, R. J.; Hughes, P.; Dodd, C.; Connell, C. R.; Heiner, C.; Kent, S. B. H.; Hood, L. E. *Nature* 1986, 321, 674-9.

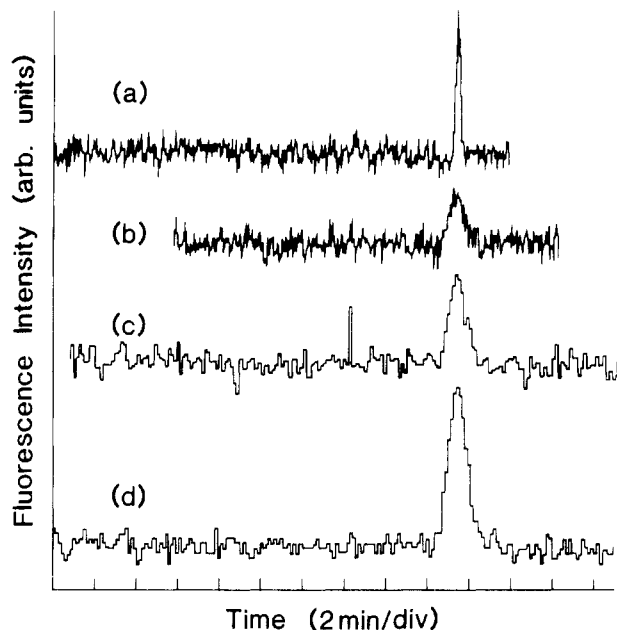


**Figure 1.** Comparison of the SNR for detection of fluorescein migrating at two different velocities before and after different velocity compensation procedures are implemented. (a) Fluorescein migrating at  $\sim 0.32$  mm/s, using an excitation intensity optimized for this migration rate and employing a data-digitization rate that generates approximately 12 points over the time needed for this band to completely pass through the detection zone. (b) Fluorescein migrating at  $\sim 0.08$  mm/s with the same excitation intensity and data-digitization rate as in panel a. Because of the slower rate of transit of this band, approximately 50 points are generated for this peak. Note the decrease in the SNR when fluorescein migrates at this slower velocity. (c) Fluorescein migrating at  $\sim 0.08$  mm/s with the same excitation intensity as in panels a and b but with a data-digitization rate scaled by the ratio of the slow-to-fast band velocities ( $= 0.08/0.32$ ) so that the peak is once again composed of approximately 12 points. (d) Fluorescein migrating at  $\sim 0.08$  mm/s with both the excitation intensity and the data-digitization rate scaled by  $0.08/0.32$ . The band in panel d receives the same amount of radiant energy and generates the same number of data points as the band in panel a, and consequently, the SNR is remaximized.

(Figure 1b). The excitation intensity is the same in both cases (but is optimized for the faster velocity), and the data-digitization rate is held constant. To explain the degradation in the signal-to-noise ratio (SNR) for the slower band, we expand upon the work of White and Stryer.<sup>7</sup> A theory is developed that relates the SNR of a fluorescence peak to excitation intensity and data-digitization rate under moderate intensity excitation conditions. This work shows that for a separation in which the excitation intensity and data-digitization rate have been optimized for a fast-traveling band, which arrives at the detection zone at a separation time of  $\tau_{\text{fast}}$ , the SNR can be maintained for all time points only if the radiant energy per band and the number of data points generated per peak are held constant. These conditions are met by continuous attenuation of the excitation intensity and of the digitization rate by a factor of  $\tau_{\text{fast}}/\tau$ , where  $\tau$  is the time elapsed since the start of the separation. Only when these two steps are taken together can the detection system exactly compensate for band velocity: all molecules are exposed to the same amount of radiant energy regardless of residence time in the detection zone, and all data points contain equivalent counts of background scatter and have a fluorescence signal proportional to analyte concentration.

Numerical analysis of the SNR reveals that compensation can prevent substantial losses in sensitivity as band velocity decreases. For the typical range of migration velocities in a CE separation, a nearly uniform SNR can be obtained without velocity compensation by using a lower than optimal excitation intensity. This approach, however, should be employed only

when measurements are not hindered by inadequate sensitivity.

In the following sections, we derive a general expression for the SNR of shot-noise-limited on-line fluorescence detection, and we compare theoretical predictions to experimental observations for CE.

## THEORY

The following assumptions are made:

1. Sensitivity is limited by shot noise in the background, which increases with the square root of the product of excitation intensity and the integration time of a data point.
2. The act of detection destroys some fraction of the analyte with first-order kinetics but does not alter whatever is responsible for the background noise.
3. All analyte species have identical photophysical characteristics (often a good approximation when analytes are tagged with the same fluorophore).
4. The proportion of molecules that occupy the triplet state is minimal, and excitation intensities are sufficiently low so that the ground electronic state remains essentially fully populated.
5. All analyte bands are characterized by the same general shape.

The effect of detection on the measurable qualities of an analyte must be examined. Most chemical detection techniques are destructive to some degree. In fluorescence detection, electronic excitation of an analyte molecule can result in photoalteration (permanent photobleaching). Branching ratios of fluorescence to photoalteration (from the  $S_1$  excited state) rarely exceed  $10^6$ .<sup>9</sup>

**A. Low Photoalteration Regime.** The degree of photoalteration during the passage of an analyte band through the detection zone dictates how much gain in integrated signal occurs when an analyte passes through the detection zone at a slower velocity. If, for example, fluorescence is measured from an analyte band traveling at a rapid velocity,  $v$ , and the intensity of excitation results in photoalteration of only 1% of analyte molecules, the fluorescence signal for the entire band can be increased approximately 2-fold by reducing the velocity to  $0.5v$ . Although the peak height will be nearly equivalent for the fast and slow bands, the temporal peak width will be greater for the slow band. Hence, the SNR for a data point integrated over the entire band will increase by approximately a factor of  $(2)^{1/2}$  in the shot-noise limit. However, on-line detection typically does not integrate the signal from an entire analyte band. In nearly all cases, a uniform data-digitization rate is employed; therefore, the number of data points produced per band scales inversely with the band velocity. The result of this procedure is that data points near the peak maximum of the slow band will have approximately the same SNR as do data points near the maximum of the fast band. (This conclusion is true only if the digitizing period is small in relation to the peak width.) Although an average of two times as much fluorescence is generated per analyte molecule in the slow band because of the increased residence time of a molecule in the detection zone, only half as many molecules pass through the detection zone during the integration period for a single data point for the slow band. Hence, in the limit of negligible analyte destruction, the fluorescence SNR remains constant, independent of analyte velocity.

**B. High Photoalteration Regime. I. Measurements on Stationary Samples.** When measurements are taken under conditions in which a large fraction of the molecules are destroyed, as would occur with more intense excitation or

(9) Soper, S. A.; Shera, E. B.; Martin, J. C.; Jett, J. H.; Hahn, J. H.; Nutter, H. L.; Keller, R. A. *Anal. Chem.* 1991, 63, 432-7.

with very slow analyte bands, the SNR does not remain constant. For a stationary (nonmoving) sample in which ground-state depletion and triplet-state pileup are negligible and the noise in the background is much larger than the noise in the signal, the radiant energy required to achieve maximal fluorescence sensitivity,  $E_{\text{opt}}$ , in a shot-noise-limited system is readily shown (see Appendix) to be

$$E_{\text{opt}} \approx (5/4)(1/\sigma\Phi_d)(\text{photons cm}^{-2}) \quad (1)$$

where  $\sigma$  is the absorption cross-section ( $\text{cm}^2 \text{molecule}^{-1}$ ) and  $\Phi_d$  is the photoalteration quantum efficiency. In this case, approximately 70% of the initial fluorescent molecules are photoaltered. Equation 1 demonstrates that for a single measurement taken on a stationary sample, the highest sensitivity can be obtained only when the sample is exposed to an optimum level of radiant energy.

**II. Measurements on Moving Analyte Bands.** Fluorescence measurements performed during chemical separations require a more complex analysis. A moving analyte band that has a nonuniform concentration profile must be sampled multiple times as it crosses the detection zone to generate an accurate peak shape. The SNR for a data point is therefore a function of more than the laser intensity and the time of excitation; it is also dependent on the concentration profile of the band and the region of the band measured during the data point. In this treatment, analyte bands are assumed to conform to a Gaussian distribution, although similar analyses could employ any well-defined peak shape. In addition, the spatial width of an analyte band is taken to be the length of the injection plug; that is, diffusion plays a minimal role in determining the band width. This is a useful assumption<sup>10</sup> and is often a reasonable approximation;<sup>8</sup> however, for instances in which diffusional broadening cannot be ignored, the present theory can be appropriately modified. We specify that an analyte band in a separation contains a total of  $N_o$  molecules. The number of molecules per unit length at distance  $x$  from the start of the detection zone at time  $t$  is

$$n_o(x,t) = \frac{N_o}{s_x(2\pi)^{1/2}} \exp\left(-\frac{[x-x_o(t)]^2}{2s_x^2}\right) \quad (2)$$

where  $s_x^2$  is the spatial variance of the band and  $x_o(t)$  is the position of the center of the band with respect to the beginning of the detection zone. Thus, in this equation,  $t = 0$  is defined as the time at which the peak maximum arrives at the start of the detection zone. We replace  $x_o(t)$  by the product of velocity and  $t$  to obtain

$$n_o(x,t) = \frac{N_o}{s_x(2\pi)^{1/2}} \exp\left(-\frac{(x-vt)^2}{2s_x^2}\right) \quad (3)$$

The detection zone length,  $L$ , is restricted to values much smaller than the band width (approximately  $6s_x$ ), which is much smaller than the distance from the starting point of the separation to the detection zone.

We have ignored thus far the disappearance of fluorescing molecules caused by photoalteration. Given our stated assumptions, the probability that a fluorescent molecule survives in a radiation field of intensity  $I$  ( $\text{photons cm}^{-2} \text{s}^{-1}$ ) to time  $t^*$  can be approximated<sup>8</sup> by

$$P(t^*) = \exp(-\sigma I \Phi_d t^*) \quad (4)$$

The time a molecule has spent within the excitation zone,  $t^*$ ,

can be related to the distance that the molecule has traveled across the excitation zone,  $x$ , and the band velocity,  $v$ , such that  $t^* = x/v$ . (In most instances, the *excitation zone* is synonymous with the *detection zone* and will be taken as such in this treatment.) Hence, the distribution of photolabile fluorescing molecules in a moving Gaussian band is

$$n(x,t) = P(t^*)n_o(x,t) = \frac{N_o}{s_x(2\pi)^{1/2}} \exp\left(-\left[\frac{(x-vt)^2}{2s_x^2}\right] - \sigma I \Phi_d x/v\right) \quad (5)$$

The rate of fluorescence is given by the product of the fluorescence rate constant ( $k_f$ ), the proportion of time a molecule spends in the excited state  $S_1$ , represented by  $\{S_1\}$ , and  $n(x,t)$ :

$$\frac{df(x,t)}{dx dt} = k_f\{S_1\}n(x,t) = \Phi_f \sigma I n(x,t) \quad (6)$$

where  $\Phi_f$  is the fluorescence quantum efficiency. Substitution of eq 5 into eq 6 yields

$$\frac{df(x,t)}{dx dt} = \frac{\Phi_f \sigma I N_o}{s_x(2\pi)^{1/2}} \exp\left(-\left[\frac{(x-vt)^2}{2s_x^2}\right] - \sigma I \Phi_d x/v\right) \quad (7)$$

The total *measured* fluorescence from the detection zone in the time window  $\delta t$  centered about time  $t$  is

$$f = K_1 \frac{\Phi_f \sigma I N_o}{s_x(2\pi)^{1/2}} \int_0^L dx \int_{t-\delta t/2}^{t+\delta t/2} dt' \exp\left(-\left[\frac{(x-vt')^2}{2s_x^2}\right] - \sigma I \Phi_d x/v\right) \quad (8)$$

where  $K_1$  is a constant that depends on the efficiency of fluorescence collection and the detector response. The excitation intensity,  $I$ , is related to the radiant energy,  $Q$ , by the square root of the band variance in time,  $Q = Is_t = Is_x/v$ . To aid in numerical integration, we define a dimensionless *radiant energy parameter*

$$\tilde{q} = \sigma \Phi_d Q \quad (9)$$

and we introduce the additional dimensionless parameters  $\tilde{t} = t/s_t = tv/s_x$  and  $\tilde{m} = x/s_x$ . The detection time window therefore can be stated as a dimensionless parameter

$$\delta \tilde{t} = \delta t/s_t \quad (10)$$

Because  $\delta \tilde{t}$  represents the number of standard deviations of a Gaussian band that passes through the detection zone within a single data point, the fraction of the total band width included in a data point is given by approximately  $\delta \tilde{t}/6$ .

We turn our attention to noise. In Poisson statistics, noise ( $\eta$ ) scales as the square root of the total number of independent events. Therefore, baseline shot-noise increases as a function of total scattered photons according to

$$\eta = K_2(I\delta t)^{1/2} = K_2(\tilde{q}\delta \tilde{t}/\sigma\Phi_d)^{1/2} \quad (11)$$

where  $K_2$  is a constant that depends on the intensity of background, the collection efficiency of background, and the detector response.

We can now write a single expression for the fluorescence SNR of a data point taken over any window  $\delta \tilde{t}$ :

$$f/\eta = [KN_o\Phi_f(\sigma/\Phi_d)^{1/2}](\tilde{q}/\delta \tilde{t})^{1/2} \times \int_0^{\tilde{m}} d\tilde{m}' \int_{\tilde{t}-\delta \tilde{t}/2}^{\tilde{t}+\delta \tilde{t}/2} d\tilde{t}' \exp\left(-\left[\frac{(\tilde{m}'-\tilde{t}')^2}{2}\right] - \tilde{q}\tilde{m}'\right) \quad (12)$$

where  $K = (2\pi)^{-1/2}(K_1/K_2)$ . Note that the excitation intensity

(10) Inclusion of analyte diffusion coefficients would expand Figure 2 into four-dimensional space (Calculation of Signal-to-Noise Ratios section) and would require that Figures 3 and 4 be depicted as three-dimensional plots. Because band broadening caused by diffusion is frequently a second-order effect (see ref 6), consideration of analyte diffusion would unnecessarily complicate the presentation of the effects of the excitation intensity and data digitization on the SNR.

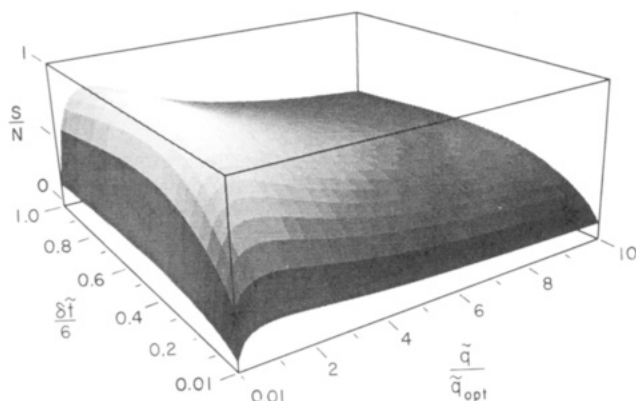


**Figure 2.** Calculated three-dimensional surface plot relating the dimensionless parameters  $\delta\bar{l}$  and  $\bar{q}$  to the fluorescence SNR for a data point centered at the middle of the Gaussian band.  $\delta\bar{l}/6$  is the fraction of the total band width integrated within the data point,  $\bar{q}$  is a parameter that scales linearly with the amount of radiant energy deposited per band, and  $\bar{q}_{opt}$  is the value of  $\bar{q}$  ( $\approx 6.3$ ) when the SNR is optimized. Note that the maximum SNR occurs at  $\delta\bar{l}/6 \approx 0.45$  and  $\bar{q}/\bar{q}_{opt} = 1$ .

and the integration window appear only in the dimensionless parameters  $\bar{q}$  and  $\delta\bar{l}$ , respectively. An immediate conclusion that can be drawn from eq 12 is that, given constant values for  $\bar{q}$ ,  $\delta\bar{l}$ , and  $\bar{n}$ , the ratio of the number of fluorescent molecules in two bands is given by the ratio of the heights of the peaks:

$$\frac{(N_o)_i}{(N_o)_j} = \frac{f_i}{f_j} \quad (13)$$

In many instances, nonfluorescent analytes are labeled with a highly fluorescent probe molecule prior to detection. In such instances, the right-hand side of eq 12 must be multiplied by a scaling parameter. In the case of analytes with one potential labeling site, this parameter can range in value from 0 to 1 and represents the fraction of analyte molecules that reacts with the fluorescent probe. For analytes that have multiple reactive sites, this parameter can be greater than 1, but does not necessarily scale with the number of tags per molecule because of fluorescence quenching effects.

### CALCULATION OF SIGNAL-TO-NOISE RATIOS

We employ standard numerical techniques to determine the relationship between  $\bar{q}$ ,  $\delta\bar{l}$ , and the fluorescence SNR from eq 12. The result is depicted in Figure 2. Here, we assume that a data point is integrated over the window  $\delta\bar{l}$ , which is centered about  $\bar{l} = 0$  (the point at which the center of the Gaussian arrives at the detection zone). The detection zone has a scaled "length",  $\bar{m} = 0.2$ , which corresponds to an excitation spot of 50  $\mu\text{m}$  with a band length of 1.5 mm ( $6s_x$ ).

The maximum in the SNR represents the point at which the infinitesimal fractional change in fluorescence signal equals the infinitesimal fractional change in noise. Using the specified system parameters, this maximum falls at  $\delta\bar{l}/6 \approx 0.45$  and  $\bar{q} \approx 6.3$ , which correspond respectively to the summation of the fluorescence from the centermost 80% of molecules in a band and an excitation intensity that results in 70% photoalteration. Although the optimal value of  $\bar{q}$  is dependent on photophysical characteristics, the optimal fraction of molecules that should be photoaltered during transit of the detection zone and the fraction that should be integrated within a single data point are independent of the photophysical parameters and the concentrations of the analytes.

Two principal factors limit employment of the long integration windows that, in theory, yield the highest sensitivity measurements. First, there is some minimum ac-

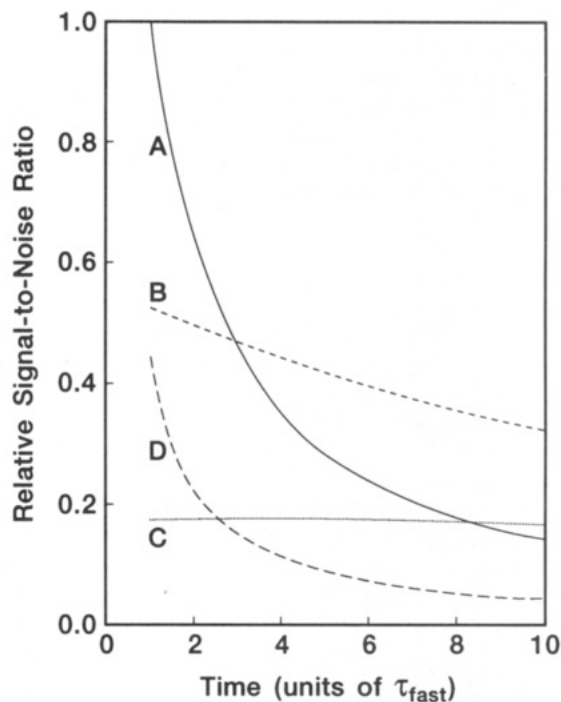


**Figure 3.** Plots relating the calculated fluorescence SNR in CE separations for bands arriving at the detection zone over a 10-fold range in separation times using a 1000-fold range in excitation intensities. A constant excitation intensity is employed for all points on the same curve. The data-digitization rate is held constant and is set to a value that generates 10 data points for the earliest detected band (at time  $\tau_{fast}$ ). Curves A–D demonstrate the effects of using an excitation intensity that is 1X, 0.1X, 0.01X, and 10X the optimal intensity, respectively, for a band arriving at the detection zone at time  $\tau_{fast}$ .

ceptable number of data points that satisfactorily defines a peak. Second, our calculation for optimal sensitivity is based on an integration window centered at the midpoint of the band, and any large deviation from this condition results in a significantly lower fluorescence signal. Generation of an intermediate number of data points per band (e.g.,  $\sim 10$ ) accurately defines most peaks, ensures that some data points will be centered closely about the true center of the band, and maintains a high SNR.

To assess the theoretical sensitivity for fluorescence measurements in CE, we assume that detection is performed during the separation process, so that an analyte band passes the detection zone at a velocity inversely proportional to the time elapsed since the separation was started. Figure 3 demonstrates the calculated sensitivity during CE separations for excitation intensities that range 1000-fold, with the excitation intensity and data-digitization rate held constant throughout each separation. The data-digitization rate is chosen so that a band arriving at the detection zone at the earliest time ( $\tau_{fast}$ ) will generate 10 data points. Arrival time of a band at the detection site is plotted along the  $x$  axis. Curve A displays the result of employing an excitation intensity necessary for optimal sensitivity at time  $\tau_{fast}$ . We refer to this intensity as  $I_{opt,fast}$ . Curves B and C show the effect of operating at 10% and 1%, respectively, of  $I_{opt,fast}$ , while curve D is the result of employing an excitation intensity that is a factor of 10 greater than  $I_{opt,fast}$ . Intensities moderately lower than  $I_{opt,fast}$  result in a less precipitous fall in the SNR and can yield better sensitivity late in a separation. Excitation intensities far below  $I_{opt,fast}$  can be employed to obtain a nearly uniform response when absolute sensitivity is not a limiting factor. Because a very small fraction of analyte molecules is destroyed during transit through the detection zone under such conditions, even at relatively late time points, the measured fluorescence per molecule continues to increase with separation time at a rate sufficient to offset

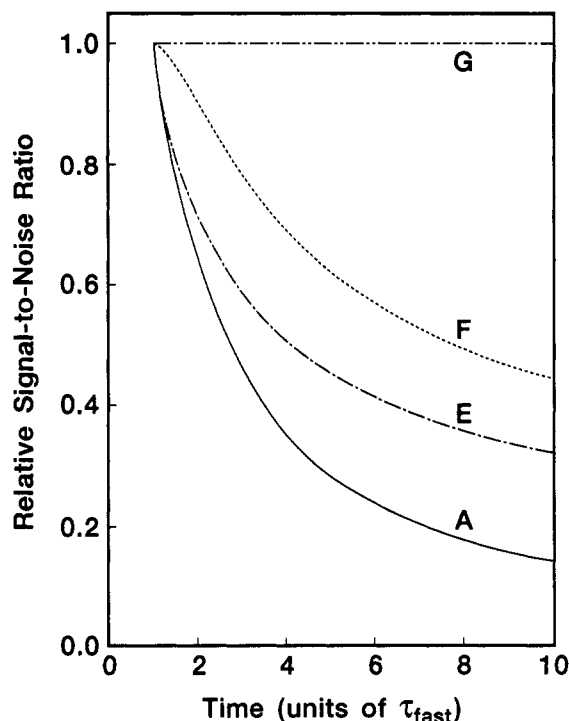


**Figure 4.** Plots relating the calculated fluorescence SNR in CE separations in which the detection system is compensated for analyte velocity through different procedures. Curve A is the result of employing no compensation, Curve E is produced by attenuating the excitation intensity by a factor of  $\tau_{\text{fast}}/\tau$ , curve F is produced by attenuating the data-digitization rate by a factor of  $\tau_{\text{fast}}/\tau$ , and curve G is produced by attenuating both the excitation intensity and the data-digitization rate by a factor of  $\tau_{\text{fast}}/\tau$ . In all cases, excitation intensity is initially optimized for time  $\tau_{\text{fast}}$ , and the data-digitization rate is chosen so that a band that arrives at the detection zone at time  $\tau_{\text{fast}}$  generates 10 points.

the loss in sensitivity that accompanies lower analyte flux through the detection zone. By using an intensity of 0.01  $I_{\text{opt,fast}}$ , a nearly flat response is seen over a factor of 10 in migration times, although the sensitivity at time  $\tau_{\text{fast}}$  is less than 20% of the maximal value. Finally, operating at an intensity greater than  $I_{\text{opt,fast}}$  results in a relatively poor SNR at the outset that rapidly worsens as the separation proceeds. These results demonstrate that sensitivity cannot be improved without limit by increasing the excitation intensity in the detection zone; an optimum intensity exists for a given migration rate. Moreover, employing intensities lower than optimal is often better than using those higher than optimal.

Ideally, a fluorescence-detection system should offer uniform response at all time points without sacrificing sensitivity. Figure 4 demonstrates the feasibility of this goal. As in Figure 3, curve A demonstrates the declining sensitivity experienced if the excitation intensity and the data-digitization rate are optimized for a band that arrives at the detection zone at time  $\tau_{\text{fast}}$  and are held constant. By attenuating excitation intensity throughout the separation by a factor of  $\tau_{\text{fast}}/\tau$  to compensate for decreasing band velocities, an improvement in sensitivity at later times is achieved (see curve E). In this case, the data-digitization rate is still held constant during the separation. Curve F shows the effect of compensating the data-digitization rate (without compensating the excitation intensity) so that all bands, regardless of residence time, generate the minimum acceptable number of data points. Compensation is accomplished by making the integration time for a data point proportional to elapsed time since the start of the separation. When both excitation intensity and the data-digitization rate are adjusted during a separation to compensate for declining band velocities, uniform sensitivity with the highest possible SNR is achieved for each peak, re-

gardless of migration velocity. This result is shown by curve G.

## EXPERIMENTAL SECTION

A laser-induced fluorescence detection system for CE was constructed to test the effects of excitation power and data-digitization rate on the fluorescence SNR. In this system, the 488-nm excitation line from an argon ion laser (Model 2017, Spectra Physics, Mountain View, CA) is focused onto a 100- $\mu\text{m}$  i.d. capillary channel (375  $\mu\text{m}$  o.d.) using a 50-mm focal length lens. The excitation zone on the capillary is placed at the focus of a 1-in. diameter parabolic mirror, identical to that described by Pentoney *et al.*<sup>11</sup> A 2-in. diameter 150-mm focal length plano-convex lens then focuses the collected fluorescence onto the photocathode of a photomultiplier tube (PMT) (Model R4632, Hamamatsu, Inc., San Jose, CA).

To minimize the collection of background, two or more 10-nm bandpass interference filters (maximum transmittance  $\approx$  60% between 545 and 550 nm) are positioned immediately in front of the collection lens. Baseline noise scales approximately with the square root of excitation intensity for the range of intensities employed in the experiments.

Typically, the laser is operated at an output of 100–200 mW and is attenuated prior to the capillary with a linear-graded neutral density filter (Melles Griot, Inc., Irvine, CA). The filter is mounted on a high-resolution translation stage to allow precise selection of the desired excitation intensity, and the intensity of the transmitted beam is measured using a power meter. The PMT is supplied with an operating voltage of 500 V when being used in a photon-counting mode and with a voltage of 600 V when being used for analog measurements.

Two different data collection systems are employed. The first system is a photon counting system (EG&G Princeton Applied Research, Princeton, NJ) that can integrate the PMT current over specified time windows. Because the degree of scatter in our system is relatively high, a series of four bandpass filters is placed before the 2-in. lens to reduce the collection of background to levels compatible with photon counting. In the second data system, the PMT current is sent to an analog charge integrator (Acton Research Corp., Acton, MA) that is programmed from a computer to bin signal over a specified time window and to relay the measurement to the computer. Because the requirement for low background is not as stringent in this case as it is with photon counting, only two bandpass filters are employed.

For all experiments, samples are introduced to a 90-cm separation capillary by placing the inlet in a sample vial raised 5 cm above the capillary outlet for 15 s. The distance from the inlet to the detection zone is 45 cm. Fluorescent derivatives of two amino acids, arginine and glutamate, are prepared separately in a pH 9.2 borate buffer (50% dimethyl formamide) using 1 mM carboxyfluorescein succinimidyl ester (Molecular Probes, Inc., Eugene, OR) and excess amino acid. Using these reaction conditions, the labeling reagent is completely consumed by reaction with arginine, although hydrolysis of the succinimidyl ester appears to compete effectively with the glutamate-succinimidyl ester reaction.

## RESULTS

In the first set of experiments we demonstrate the general validity of the theory by measuring the fluorescence SNR for a single compound, fluorescein, that traverses the detection zone at two velocities differing by a factor of 4 in magnitude. The photon counting system is employed in these experiments. In the first separation, shown in Figure 1a, a plug of fluorescein is electrophoresed using a voltage of 9 kV in a 5 mM disodium phosphate buffer. Under these conditions, the time between the injection of fluorescein and its arrival at the detection zone is  $\tau_{9\text{kV}} \approx 23.7$  min, which corresponds to a velocity of  $v_{9\text{kV}} \approx 0.32$  mm/s. Here, excitation intensity is optimized to yield the highest possible SNR which is observed to result in approximately 70% photoalteration of fluorescein ( $I_{\text{opt, 9kV}} \approx$

(11) Pentoney, S. L., Jr.; Konrad, K. D.; Wilbur, K. *Electrophoresis* 1992, 13, 467–74.

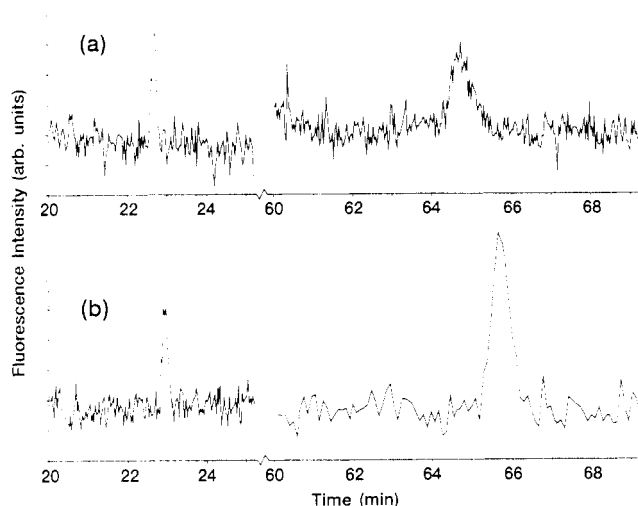


**Figure 5.** Separations of two fluorescein-labeled amino acids demonstrate the effect of velocity compensation on the SNR. (a) A separation of fluorescein-arginine ( $\tau_{\text{arg}} \approx 22.6$  min.) and fluorescein-glutamate ( $\tau_{\text{glu}} \approx 64.7$  min.) (concentrations are given in the text). Excitation intensity is optimized for the fast-migrating fluorescein-arginine and is kept constant throughout the separation. The data-digitization rate is chosen to generate approximately 10 points for the fluorescein-arginine peak and is also kept constant during the separation. Note that the glutamate peak is barely detectable. (b) A repeat of the separation in panel a, except that the excitation intensity and the data-digitization rate are optimized for both peaks by attenuating these parameters by the ratio of the velocity of the fluorescein-glutamate band to the velocity of the fluorescein-arginine band following the detection of fluorescein-arginine. The fluorescein-glutamate peak is now easily detected.

45 mW). The data integration time is set to 2 s to produce approximately 12 points per peak. In the separation shown in Figure 1b, all conditions remain identical to those used for Figure 1a, except that the separation voltage is reduced to 2.5 kV, which decreases the fluorescein velocity to 26% of its initial value ( $v_{2.5\text{kV}} \approx 0.08$  mm/s). (Although the velocity for fluorescein should ideally scale as the separation voltage, a number of voltage-dependent phenomena can upset this relationship.) Note the increase in temporal band width because of slower migration through the detection zone. To minimize differences in spatial band width that may be induced by diffusion, a high field setting (200 V/cm) is utilized until the band nears the detection zone. The capillary voltage is then reduced to 2.5 kV for the remainder of the separation. Comparing panel a to panel b in Figure 1, the SNR decreases by more than a factor of 2.5, which agrees well with theory.

By scaling the data-digitization rate by a factor of  $v_{2.5\text{kV}}/v_{9\text{kV}}$  ( $= 0.26$ ), the loss in sensitivity can be partially reversed. This effect is shown in Figure 1c. Complete recovery of the fluorescence SNR is achieved by scaling the data-digitization rate and the excitation intensity in concert, which is demonstrated in Figure 1d.

The applicability of these concepts to measurements performed on *different* analyte species derivatized with the same fluorescent probe is shown in Figure 5. For these measurements, the analog charge integrator is used. To enhance the differences in migration velocity of fluorescein-arginine and fluorescein-glutamate, we employ a 25 mM borate buffer (pH 7.6) with 30% methanol content by volume. Excitation intensity is initially optimized for fluorescein-arginine migrating in a separation field of 200 V/cm ( $I_{\text{opt, arg}} \approx 35$  mW), and the data-integration period (2 s) is selected to yield approximately 10 points for this peak. Figure 5a displays a separation of fluorescein derivatives of arginine ( $4 \times 10^{-11}$  M) and glutamate ( $4 \times 10^{-10}$  M) using these conditions. (The actual concentration of fluorescein-glutamate is significantly lower than this nominal value because of the poor

efficiency of the glutamate labeling reaction.) Both species are present close to the detection limit (SNR  $\approx 2.5$ ). In a second separation of the labeled amino acids, shown in Figure 5b, the excitation intensity and data-digitization rate are scaled to the detection time of each band by decreasing both parameters by a factor of 2.8 after the detection of fluorescein-arginine. These corrections yield an improvement by approximately a factor of 2 in the SNR for fluorescein-glutamate.

## CONCLUSION

These results show that the fluorescence SNR for a band can be dramatically affected by the velocity at which it transits the detection zone. Thus, continuous manipulation of excitation intensity and data-digitization rate should be considered whenever detection is performed on-line, where analytes are still undergoing separation from one another. Such instances are not limited to capillary electrophoresis.

For instances in which all bands migrate at similar velocities, little variation will occur in the SNRs, and compensation for band velocity may be unnecessary. There are, however, numerous instances in which species migrate at significantly different rates and are measurable only by using *optimized* conditions. In such cases, compensation for differences in analyte velocity are essential in detection and quantitation.

## ACKNOWLEDGMENT

We gratefully acknowledge the helpful advice and assistance of Neil Shafer. In addition, we thank Beckman Instruments, Inc., and the National Institute of Mental Health (Grant No. NIH 5R01 MH45423-03) for continued financial support. J.B.S. is a Howard Hughes Medical Institute Predoctoral Fellow.

## APPENDIX

Begin by assuming that almost all molecules occupy the ground state  $S_0$ , that negligible triplet-state accumulation occurs, and that the noise in the background is much larger than the noise in the signal. To a good approximation, the rate equation for fluorescence then simplifies to  $df/dt^* = \Phi_f k_a N_0 \exp(-k_a \Phi_d t^*)$ , which integrates to

$$f(t^*) = \frac{K_1 \Phi_f N_0}{\Phi_d} [1 - \exp(-\sigma I \Phi_d t^*)]$$

Shot-noise accumulates as

$$\eta(t^*) = K_2 (I t^*)^{1/2}$$

If we let  $(I t^*) = E$ , the total radiant energy (in units of photons  $\text{cm}^{-2}$ ), and  $\sigma \Phi_d = \beta$ , the signal to noise varies with  $E$  as

$$\frac{f}{\eta} = \frac{K_1 \Phi_f N_0}{K_2 \Phi_d} [1 - \exp(-\beta E)] E^{-1/2}$$

The highest signal-to-noise ratio occurs when  $d(f/\eta)/dE = 0$ . This equation can be solved using Newton's iterative method to yield the optimal radiant energy input:

$$E_{\text{opt}} = \frac{1.256}{\beta} \approx (5/4) \frac{1}{\sigma \Phi_d}$$

Substitution of  $E_{\text{opt}}$  for  $(I t^*)$  in eq 4 in the main text demonstrates that the maximum SNR is achieved when approximately 70% of the molecules are photoaltered.

RECEIVED for review May 10, 1993. Accepted July 25, 1993.\*

\* Abstract published in *Advance ACS Abstracts*, September 15, 1993.